NUMERICAL MODELING OF SOLAR REACTOR FOR WATER TREATMENT: HYDRODYNAMIC, KINETIC AND SOLAR IRRADIATION ASPECTS

L. Aoudjit, A. Sebti,F. Madjene, H. Lebik, B. Boutra, S. Igoud
Unité de Développement des équipements Solaires, UDES /Centre de Développement des Energies Renouvelables, CDER, Bou Ismail, 42415, W. Tipaza, Algérie

ABSTRACT

Mathematical modelling have emerged over the past two decades as one of the key tool for design and optimize performances of physical and chemical processes intended to water disinfection. Water photolysis is an efficient and economical technique to reduce bacterial contamination. It exploits the germicidal effect of solar or artificial UV light to inactivate pathogenic microorganisms. In this work we propose a state of art about kinetic, hydrodynamic and solar irradiation models used to simulate solar reactor for water disinfection and an example of a simulation study performed by Fluent Software.

KEYWORDS: *Water photolysis, Numerical simulation, solar reactor*

I. INTRODUCTION

Numerical modeling and simulation are indispensable tools to improve performance of solar reactor for water disinfection and contribute to the development of new processes. Solar water disinfection or photolysis is an old process which exists since 1910th, but it's only from 1970th that researchers have interested to understand the mechanism governing the destruction of pathogenic microorganisms by solar irradiation. When contaminated water is exposed to natural or artificial ultraviolet irradiation, UV will break the molecular bonds within microorganism's DNA and destroy them, rendering them harmless or prohibiting growth and reproduction. Time required to achieve a total disinfection depends both on the quality of water and the intensity of irradiation. The kinetic of disinfection or bacterial response to UV irradiance have been described by several models. The basic model is the Chick-Watson model where a pseudo first order rate expression was established and in which the overall rate of photo reaction is directly proportional to UV intensity and exposure time. Several elaborated expression of disinfection kinetic are developed later. It gave best results for the description of UV disinfection than Chick-Watson model. The design of photo-reactor operating in continuous disinfection system, required tacking in account the hydrodynamic behavior of water in the reactor. Since the kinetic of disinfection depends on irradiation intensity distribution, coupling the hydrodynamic and solar radiation distribution is of crucial importance. In this work we propose a numerical simulation study for hydrodynamic and solar irradiation distribution in a tubular photo-reactor. The radiative transfer equation (RTE) in conjunction with momentum conservation equations were solved using the CFD code Fluent under the assumption of three-dimensional incompressible flow in unsteady turbulent regimes. The discrete ordinate model (OD) was used to simulate the light intensity distribution inside the reactor while Reynolds Averaged Navier-Stocks equations (RANS), the most widely used approach for calculating fluid flow field, were closed by one equation model namely Large Eddy Simulation. The results of simulation concerned radiation, temperature,

International Journal of Scientific Research and Management Studies (IJSRMS)
ISSN: 23493771 **Volume 1 Issue 12, pg: 422-443**

turbulence and velocity fields are discussed and the effect of inclination angle of reactor relative to the horizontal is investigated.

II. MODELING SOLAR REACTOR FOR WATER DISINFECTION

Solar water disinfection is a sustainableprocess for the removal of pathogenic micro-organisms. In fact, compared to traditional treatment using chemicals additives like chlorine and ozone, solar disinfection does not alter taste or composition of water and reduces pollution without the formation of disinfection by-products which are harmful to human.Solar reactor are systems that expose flowing water to UV light received from sun or produced by lamp. In order to ensure that UV reactors provide sufficient decontamination rates, design and operating regimes must be properly optimized by means of experimental or numerical models. Numerical models that simulate the disinfection process of UV system involve fluence rate models for UV light intensity distribution, turbulence models for flow field prediction, and microbial inactivation kinetic models.

2.1.Kinetic modeling of solar reactor for water disinfection

Kinetic models for solar disinfection are derived from the earlier linear model developed by Chick and Watson in 1908 to describe the inactivating action of a chemical disinfectant on micro-organisms. Germicidal UV light which ranges from 200 nm to 400 nm inactivates microorganisms by damaging deoxyribonucleic acid (DNA) and ribonucleic acid (RNA) and causes faults in the transcription of genetic information. Microorganisms continue to live but it cannot reproduce.

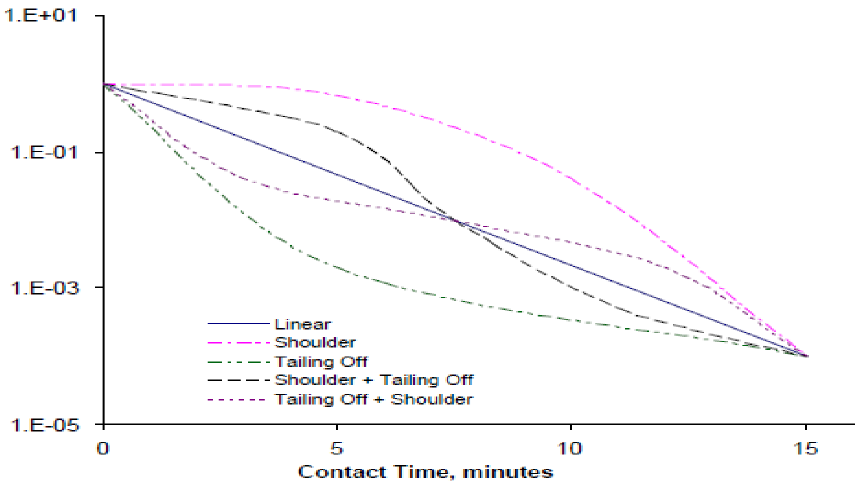

Figure 1. Microorganisms inactivation kinetic profiles

Inactivation rates as represented in the figure above show derivations from Chick Watson model. In fact, rates of kill have been found to increase with time in some cases and to decrease with time in other cases.
Principle inactivation models developed to account for these derivations are summarized below:

Table 1. Kinetic models for water disinfection

Model	Related equation	Parameters	Observation
Chick – Watson (1908)	$\ln\frac{N}{N_0} = -k^{'}C^n t$	K': Pseudo-first order reaction kenitic N_0,N: Number of survival micro-organisms at time t_0 and time t respectively n: Coefficient of dilution	Linear model C: chemical desinfectant concentration or solar radiation intensity

Model	Related equation	Parameters	Observation
Hom(1972)	$\ln\frac{N}{N_0} = -k^{'}C^{n}t^{m}$	m=1, Chick – Watson model *m>1, Curve with shoulder *m<1, Curve with tailling off	m: empirical parameter which explain derivations from Chick-Watson model
Series events proposed by Severin (1984)	$\ln\frac{N}{N_0} = -k^{'}Ct + \ln\left(\sum_{i=0}^{n-1}\frac{(kct)^{i}}{i!}\right)$	k: Second order reaction rate, i: Integer representing the lethal number of reactions for a single organism	The microorganism is inactivated after a series of reactions. this model propose that ***i*** interactions between microorganism and disinfectant are required until total disinfection is reached.
Several models exist in which expression of inactivation rates is more elaborated. We can list: Hass model (1998), Target model, multi target model,....			

2.2. Hydrodynamic modeling of photo-reactor

Two general approaches are usually taken to model hydrodynamic or flow field in UV disinfection reactor depending on whether micro-organismparticlesare treated as continuous phase or discrete phase. In the first approach "Euler-Euler framework", particle phase is considered as continuum for which equations representing the conservation of mass and momentum are solved as well the fluid phase (water). In the second approach "Euler-Lagrange framework", water is treated as fluid phase also while for the particle phase, we should track over time the pathway of each individual particle. It's Clair, that the first approach is less complicated than the second one which needs a static study of all particles' trajectories. In our study we will adopt the Euler-Euler framework because of the small size of microorganisms which for all practical purposes can be assumed to follow the motion of fluid. Several hydrodynamic models are available. Selecting of the adequate model able to describe the fluid motion in a reactor needs a good comprehension of physical phenomena. Hydrodynamic models are based on the resolution of Reynolds Averaged Navier Stocks Equations (RANS) which, for incompressible flows, can be expressed by:

$$\frac{\partial u_i}{\partial x_i} = 0 \qquad (1)$$

$$\rho\frac{\partial u_i}{\partial t} + \rho u_j\frac{\partial u_i}{\partial x_j} = -\frac{\partial p}{\partial x_i} + \frac{\partial}{\partial x_j}\left[\mu\left(\frac{\partial u_i}{\partial x_j} + \frac{\partial u_j}{\partial x_i}\right)\right] - \rho\frac{\partial}{\partial x_j}\left(\overline{u_i^{'}u_j^{'}}\right) \qquad (2)$$

Table 2. Hydrodynamic models

Model	Related equation
Standard *k*-*ε* model or Two equations model	Kinematic eddy viscosity $u_t = \rho \frac{C_\mu k^2}{\varepsilon}$ Turbulence Kinetic Energy $\frac{\partial k}{\partial t} + \overline{u}_j \frac{\partial k}{\partial x_j} = v_t \left(\frac{\partial \overline{u_i}}{\partial x_j} + \frac{\partial \overline{u_j}}{\partial x_i} \right) \frac{\partial \overline{u_i}}{\partial x_j} + \frac{\partial}{\partial x_j} \left[\left(v + \frac{v_t}{\rho_k} \right) \frac{\partial k}{\partial x_j} \right] - \varepsilon$ Dissipation rate : $\frac{\partial \varepsilon}{\partial t} + \overline{u}_j \frac{\partial \varepsilon}{\partial x_j} = C_{\varepsilon 1} \frac{\varepsilon}{k} u_t \left(\frac{\partial \overline{u_i}}{\partial x_j} + \frac{\partial \overline{u_j}}{\partial x_i} \right) \frac{\partial \overline{u_i}}{\partial x_j} - C_{\varepsilon 2} \frac{\varepsilon^2}{K} + \frac{\partial}{\partial x_J} \left[\left(v + \frac{v_t}{\rho_k} \right) \frac{\partial \varepsilon}{\partial x_j} \right]$ The empirical constants used in this model are: $C_{\varepsilon 1} = 1.44, C_{\varepsilon 2} = 1.92, C_\mu = 1.92, \rho_k = 1.0, \rho_k = 1.3$
***k*-*ε* *RNG* model**	In this model, the eddy viscosity, k and ε are still given by equations. However, the coefficient $C_{\varepsilon 2}$ is modified and defined by: $C_{\varepsilon 2} = C_{\varepsilon 2} + \frac{C_u \lambda^3 \left(1 - \frac{\lambda}{\lambda_0} \right)}{1 + \beta \lambda^3}$ Where, $\lambda = \frac{k}{\varepsilon} \sqrt{2 S_{ij} S_{ji}}\ ,\ S_{ij} = \frac{1}{2} \left(\frac{\partial \overline{u_i}}{\partial x_j} + \frac{\partial \overline{u_j}}{\partial \overline{x_i}} \right)$ The empirical constants used in this model are: $C_{\varepsilon 1} = 1.42, C_{\varepsilon 2} = 1.68, C_\mu = 0.085, \rho_k = 0.72, \beta = 0.012, \lambda_0 = 4.38$
$k\omega$ ***Model***	Kinematic eddy viscosity $u_t = \frac{k}{\omega}$ Turbulence Kinetic Energy $\frac{\partial k}{\partial t} + \overline{u}_j \frac{\partial k}{\partial x_j} = v_t \left(\frac{\partial \overline{u_i}}{\partial x_j} + \frac{\partial \overline{u_j}}{\partial x_i} \right) \frac{\partial \overline{u_i}}{\partial x_j} + \frac{\partial}{\partial x_j} \left[\left(v + \rho^* v_t \right) \frac{\partial k}{\partial x_j} \right] - \beta^* k \omega$ Specific dissipation rate : $\frac{\partial \omega}{\partial t} + \overline{u}_j \frac{\partial \omega}{\partial x_j} = \alpha \frac{\omega}{k} u_t \left(\frac{\partial \overline{u_i}}{\partial x_j} + \frac{\partial \overline{u_j}}{\partial x_i} \right) \frac{\partial \overline{u_i}}{\partial x_j} + \frac{\partial}{\partial x_J} \left[\left(v + \rho v_t \right) \frac{\partial \omega}{\partial x_j} \right] - \beta \omega^2$ The empirical constants and auxiliary relations are defined as: $\beta = 0.09, \rho = 0.5, \rho^* = 0.5, \alpha = 5/9, \beta = 3/40$

Large Eddy Simulation (LES)	The most used model for simulating turbulent flows for complex geometries. LES is based on the definition of a "filtering operation" where velocity field is divided into : 1. Resolved part, represents the large scale motions or eddies, can be discretized and solved numerically on a computational mesh (Filtered Navier -Stocks equations;) 2. Unresolved part, represents small scale motions, cannot be adequately solved on a computational mesh (Sub-grid scale) and needs to be modeled. The resolved part of the velocity field is governed by : $\frac{\partial \overline{u_i}}{\partial x_i} = 0;$ $\frac{\partial \overline{u_i}}{\partial t} + \frac{\partial}{\partial x_j}(\overline{u_i}\,\overline{u_j}) = -\frac{1}{\rho}\frac{\partial \overline{p}}{\partial x_i} - \frac{\partial \tau_{ij}}{\partial x_j} + \nu \frac{\partial^2 \overline{u_i}}{\partial x_i \partial x_j}$ While the sub-grid scale stress is governed by : $\tau_{ij} = \overline{u_i u_j} - \overline{u_i}\,\overline{u_j}$; This expression takes account the effect of small scales motions on the fluid behavior. Since1963, several mathematical expressions were developed to model the sub-grid scale stress 1. Smagorinsky model (1963) 2. Algebraic dynamic model (19991) 3. Loclized Dynamic model (1993) 4. WALE (Wall-Adapting Local Eddy-viscosity) (1999) 5. Dynamic Global Coefficient model (2007)

The last term in the right side of equation (2) is the Reynolds stresses and it describes the turbulent fluctuations of fluid. It can be related to the mean velocity gradients by:

$$-\rho\left(\overline{u_i^{'}u_j^{'}}\right) = u_t\left(\frac{\partial u_i}{\partial x_j} + \frac{\partial u_j}{\partial x_i}\right) - \frac{2}{3}\rho k \quad \text{Boussinesq approximation}$$

Where :

$u_t = \rho C_u \frac{k^2}{\varepsilon}$ is the turbulent viscosity, k is the turbulent kinetic energy and ε is the turbulent dissipation rate. The resolve of equations (1) and (2) requires introducing additive equation in order to modeling the Reynolds stresses and predicting turbulence phenomena.

That's why turbulent flows can be modeled in a variety of ways. The most common models are:

The complex geometry of the photo-reactor and the presence of elbows in the computational domain require the use of Large Eddy Simulation (LES/WALE).

2.3. Modeling UV light intensity

In disinfection reactors, UV light is received by sun or produced by artificial lamp. Fluence rate is the spatial distribution of UV light intensity inside the photo-reactor. Fluence rate can be predicted by several models.

2.3.1. Discrete ordinate model

Discrete ordinate method is one of the numerical approaches for solving the radiation transfer equation (RTE) which is the most model used to predict the fluence rate of natural irradiation. In fact, solar irradiation distribution in an absorbing and scattering media is governed by:

$$(\Omega.\nabla)I(r,\Omega) = -(k_a + k_s)I(r,\Omega) + k_a I_b(r) + \frac{k_s}{4\pi}\int_{\Omega'=4\pi} I(r,\Omega')\Phi\left(\Omega' \rightarrow \Omega\right)d\Omega'$$

Where;
Ω Direction of propagation of radiation of radiation beam
k_a, k_s Absorbing and scattering coefficient (l/m)
I_b, Intensity of black body radiation
Φ, Scattering phase function
$(\Omega.\nabla)I(r,\Omega)$: Gradient of intensity along propagation direction
$(k_a + k_s)I(r,\Omega)$: Lost due to absorption and to out- scattering respectively
$k_a I_b(r)$: Gain due to black body emission
$\frac{k_s}{4\pi}\int_{\Omega'=4\pi} I(r,\Omega')\Phi\left(\Omega' \rightarrow \Omega\right)d\Omega'$ Gain due to in-scattering

2.3.2. UV lamp models

Several models have been implanted to simulate and characterize the fluence rate produced by a UV lamp. These models include:

Table 3. Incident radiation models

Model	Approach	Related equation
Multi Point Source Summation (MPSS)	Based on the assumption that the emission of a linear lamp is equivalent to that of n point sources of the lamp. Model takes on account the effect of reflection, absorption and refraction phenomena	$I_A = (1-R_1)(1-R_2)\frac{P/n}{4\pi(d_1+d_2+d_3)^2}T_w^{d_3/0.01}T_q^{d_2/0.01}Focus$ Where; P : Output power emitted by the lamp; n: Number of point sources; R_1, R_2: Reflectance factors for the air/quartz and quartz/air interfaces; T_w, T_q: Transmittance of water and quartz; d_1, d_2, d_3,Path lengths of UV light; Focus: Refraction effect;
Multi Segment Source Summation (MSSS)	Based on the MPSS model; Model takes on account the effect of refraction angle	$I_A = (1-R_1)(1-R_2)\frac{P/n}{4\pi(d_1+d_2+d_3)^2}T_w^{d_3/0.01}T_q^{d_2/0.01}Focus\theta_1$
Line Source Integration (LSI)	Based on the MSSS model; The number of point sources n approaches ∞;	$I = \frac{p}{4\pi LR}\left[\left(\arctan\frac{L/2+H}{R}\right)+\arctan\left(\frac{L/2-H}{R}\right)\right]$ Where, R: Normal distance from a lamp of a point ; H: Longitudinal distance from the center of the lamp; L: Length of the lamp;

In our study we have exploited the germicidal effect of sunlight. That's why the adequate model to predict fluence rate is the discrete ordinate method.

III. NUMERICAL MODELING AND SIMULATION SOFTWARE

The numerical modeling and simulation of water photo-reactor was performed using the Computational Fluid Dynamic software "Ansys Fluent 6.3.26" which predicts fluid flow, heat and mass transfer, chemical reactions, and related phenomena by solving the set of governing mathematical equations:

- Conservation of mass
- Conservation of momentum
- Conservation of energy
- Conservation of species
- Effects of body forces

Fluent is a useful tool to:

- Concept and study of new process,
- Develop existing process,
- Diagnosis and resolve anomalies, by reducing total effort and cost required for experimentation and data acquisition.

Solution of partial differential equations expressing hydrodynamic, radiative and chemical reaction rate using CFD tool is based on finite volume method and includes three (03) steps:

- Pre-processing,
- Solver,
- Post-processing.

a.* Pre-processing*: is the first step in building and analyzing a flow model which involves:

- Definition of the domain of computation or the geometry of reactor,
- Meshing or grid generation : discretization of the reactor into a finite set of control volumes ,
- Definition of fluid proprieties,
- Specification of boundary conditions.

GAMBIT is the pre-processing for CFD Fluent.

b. Solver: partial differential equations arediscredited into a set of algebraic expressions through which mass, momentum and energy transport are predicted at discrete points in the domain of computation. Resolution of algebraic equations is carried out in Fluent by finite volume method.

c. Post-processing: is the final step in CFD analysis, involves organization and interpretation of the predicted flow data and production of CFD image (velocity profile, temperature profile, pressure profile, radiation profile, turbulence zones).

IV. NUMERICAL STUDY OF THE TUBULAR PHOTO-REACTOR

4.1 Description of experimental reactor

Experiments of solar water disinfection were performed during April 2012 in the Development Unit of Solar Equipments situated at 30 Km west of Algiers using a tubular photo-reactor consisting of five (05) Pyrex glass tube assembled in series and inclined at 36° relative to the horizontal.

This tubular photo-reactor is designed to decontaminate 30 liters of secondary treated wastewater with a flow rate of 0.001 liters/mn.

Figure 2. Experimental prototype (Tubular photo-reactor)

4.2 Geometric configuration and grid generation of the tubular photo-reactor

Employing the software Gambit, three dimensional geometry of the tubular photo-reactor was created. In order to provide the sufficient control volumes for the CFD simulation in Fluent and good convergence of hydrodynamic and radiation results, the computational domain was discretized with all hexahedral elements. 269 788 meshes were generated and exported to be read by Fluent.

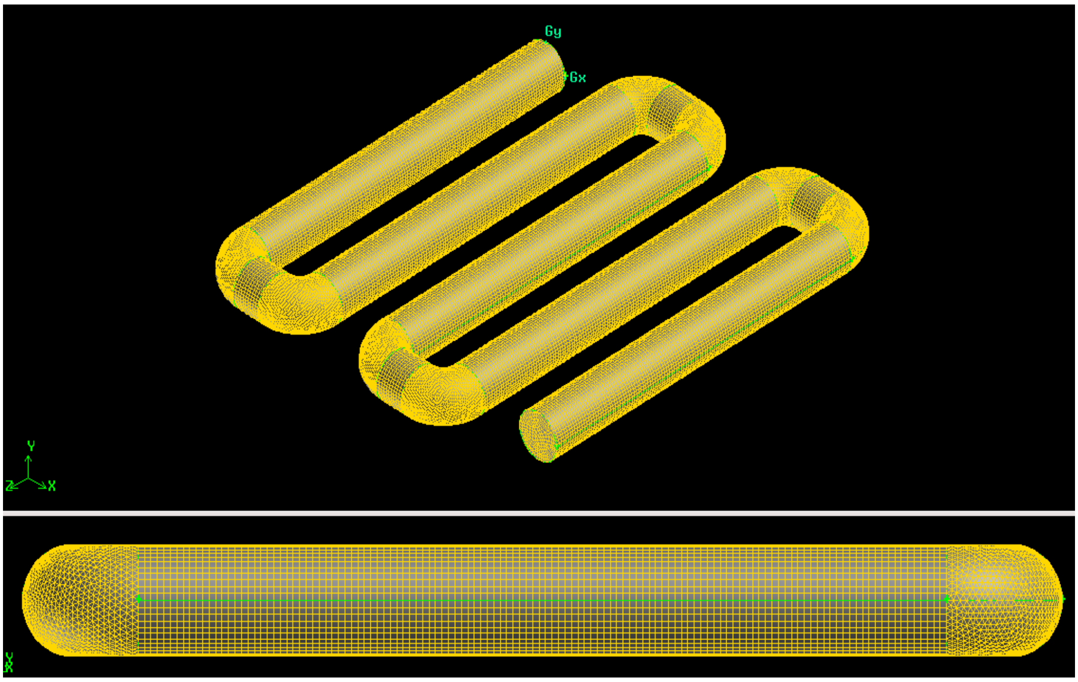

Figure 3. Geometric configuration of the tubular photo-reactor

ISSN: 23493771 Volume 1 Issue 12, pg: 422-443

4.3 Results of simulation study performed by Fluent

Wastewater was exposed to solar irradiation during 06 hours (from 09 pm to 03 pm). Intensity of irradiation ranged from 780 to 1480 w/m^2. The variation of wastewater's temperature as a function of intensity of irradiation for horizontal and inclined photo-reactor (α=36°, α=45°) is presented below.

4.3.1. Discussion

It's noticeable that wastewater temperature depends on the intensity of solar irradiation and increases over exposure time for both horizontal and inclined photo-reactors.
As shown on temperature profiles plotted below, in some parts of tubular photo-reactor, like elbows, the raise of wastewater temperature is more appreciable than other parts like tubes (made of Plexiglas). In fact, elbows are made of Polyvinyl Chloride (PVC) which is more thermal conductive than Plexiglas. So heat flow spreads from elbows to the bulk of reactor.

4.3.2. Temperature profiles

Horizontal photo-reactor (α=0°) Irradiation 780 W/m²		
80 s	120 s	180 s

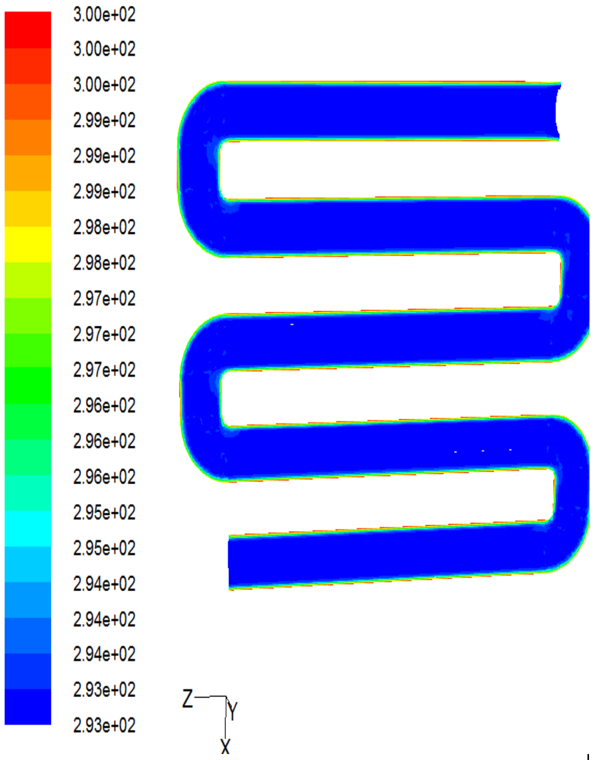

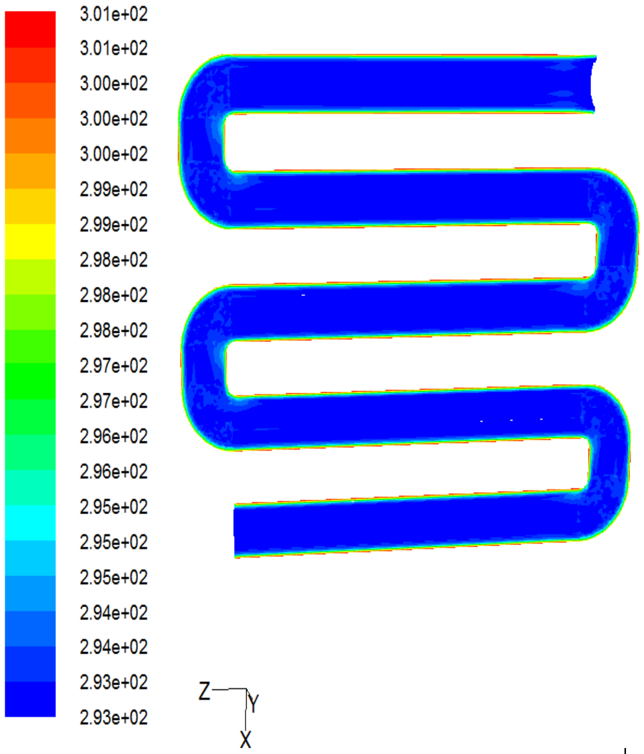

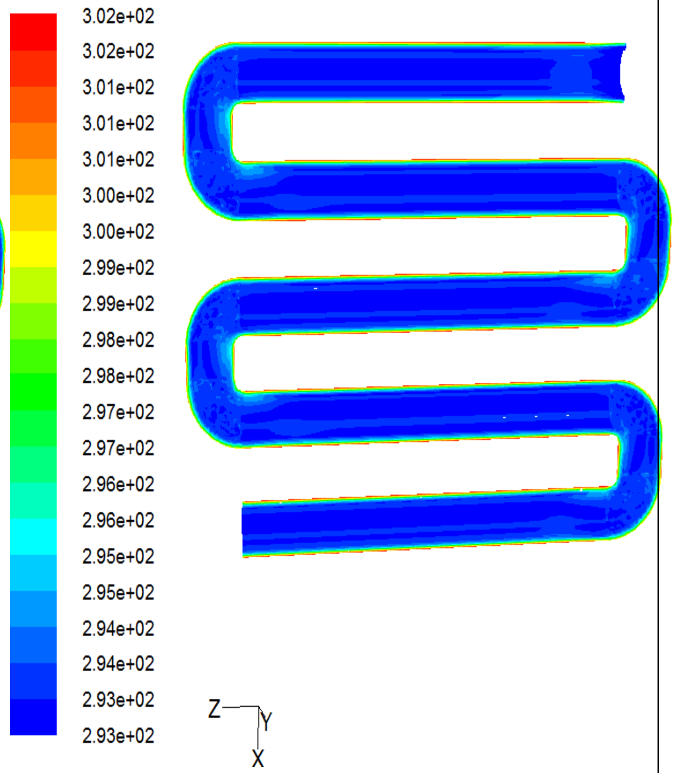

Horizontal photo-reactor (α=0°)
Irradiation 1480 W/m²

80 s

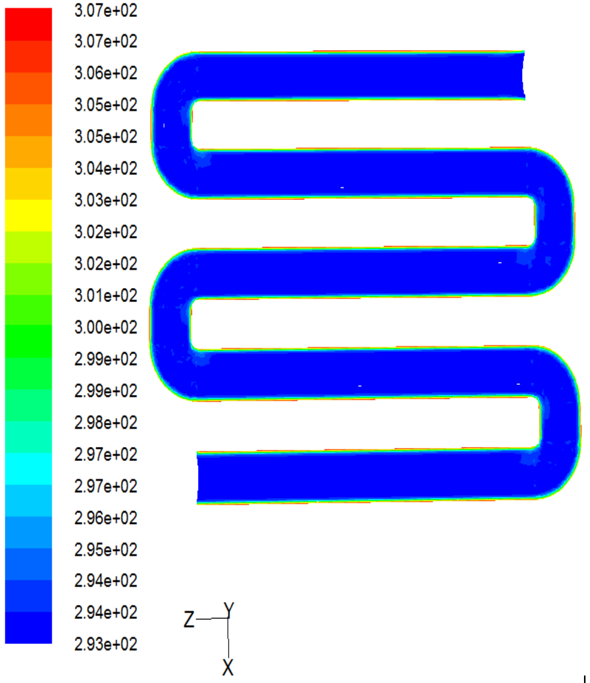

120 s

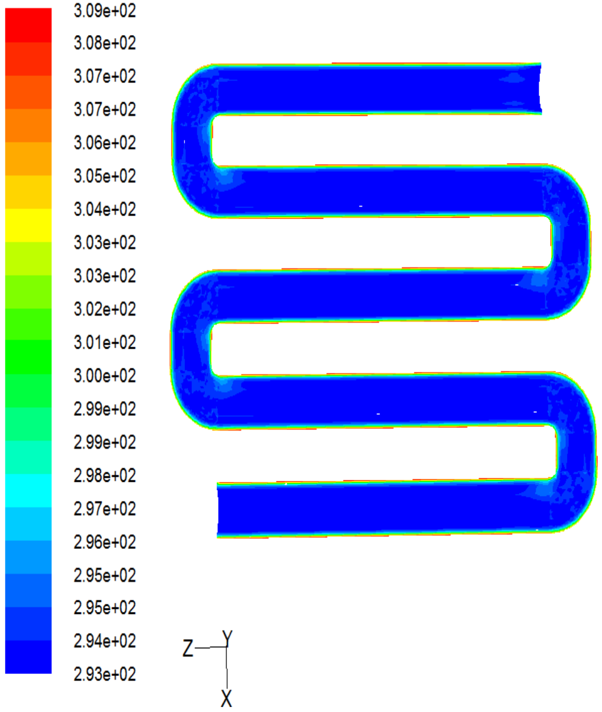

180 s

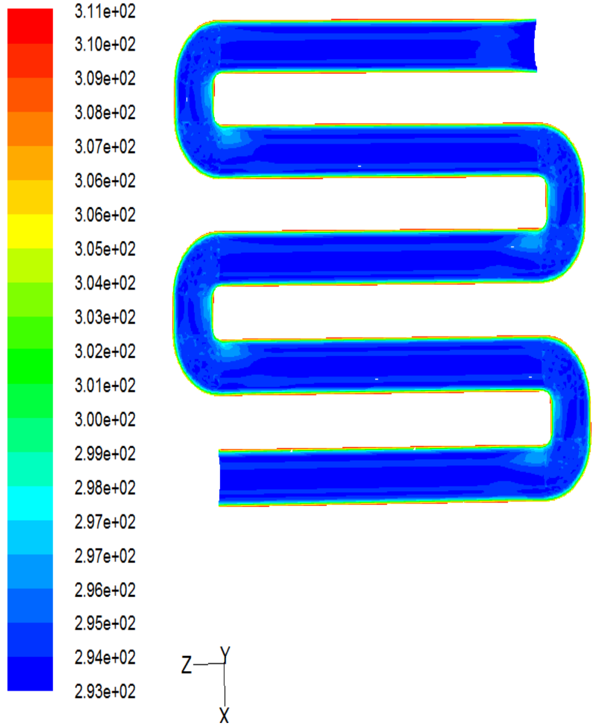

Horizontal photo-reactor (α=0°) **Irradiation 780 W/m²**

80 s

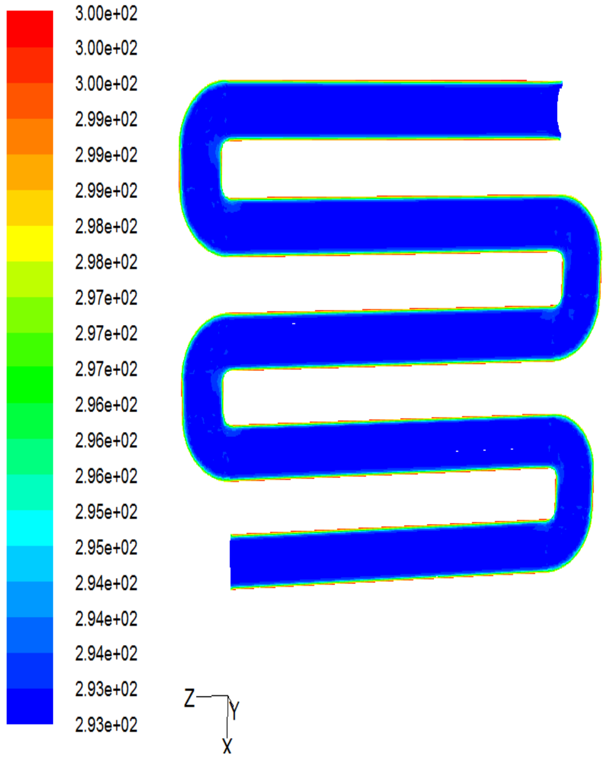

120 s

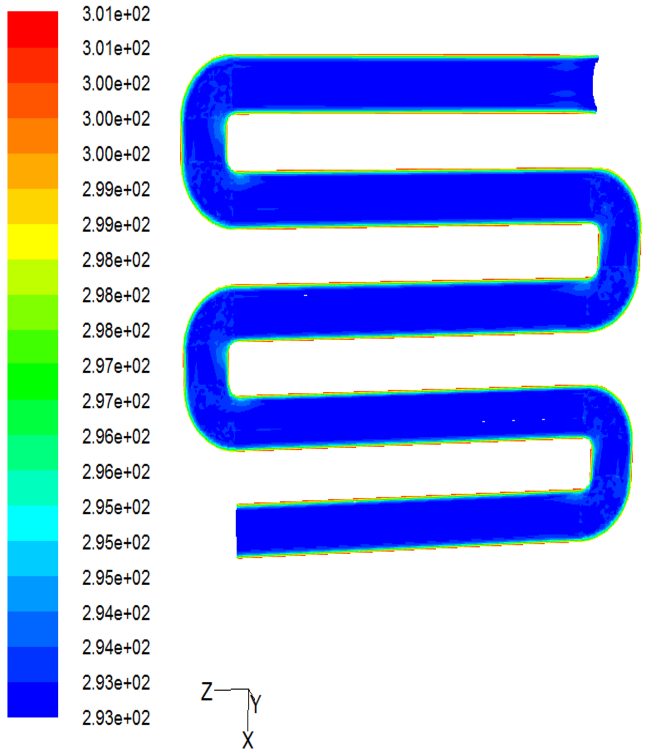

180 s

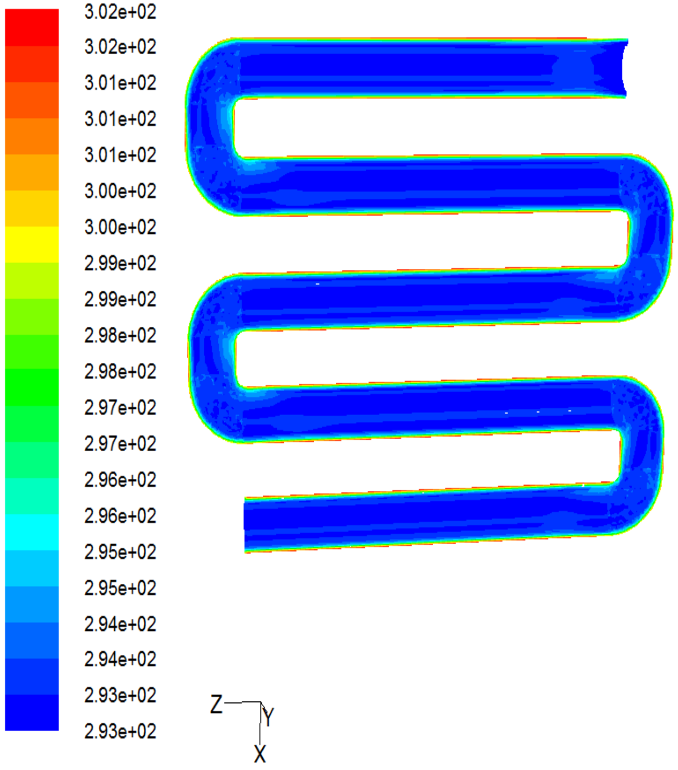

Horizontal photo-reactor (α=0°) **Irradiation 1480 W/m²**

80 s	120 s	180 s
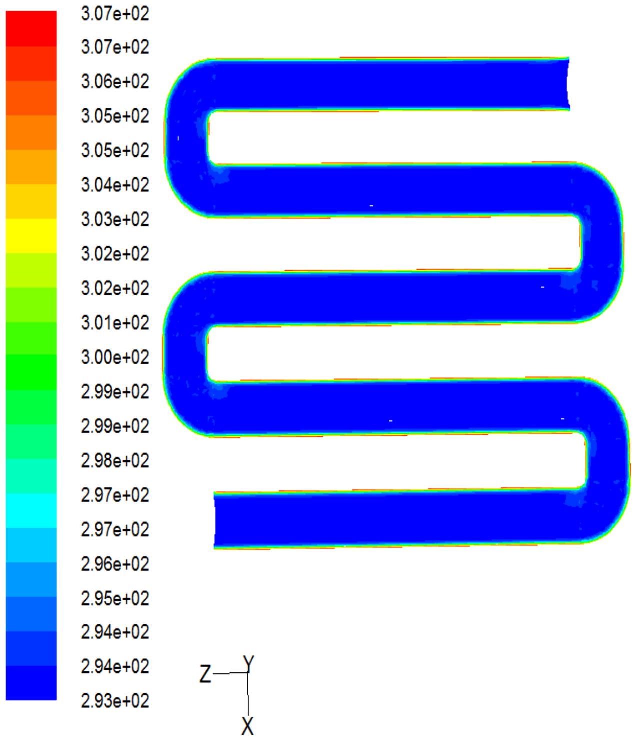	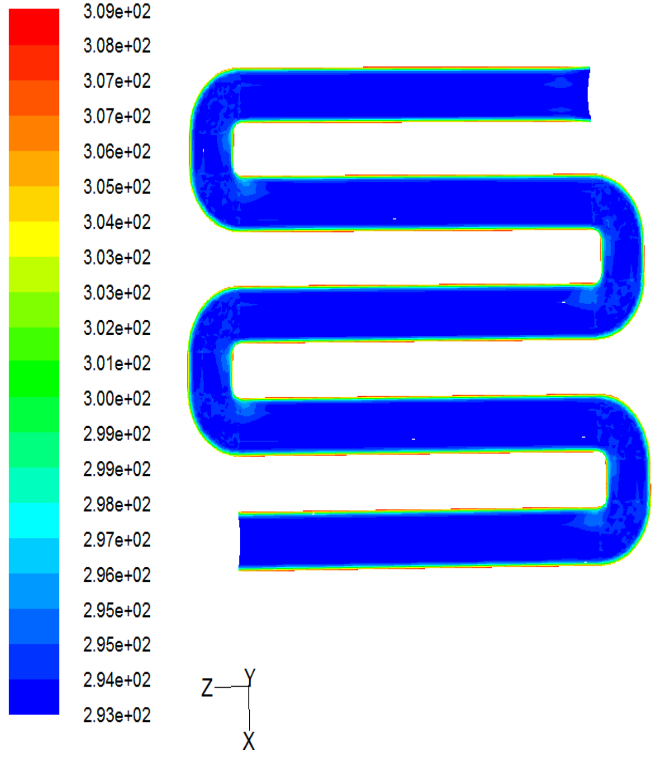	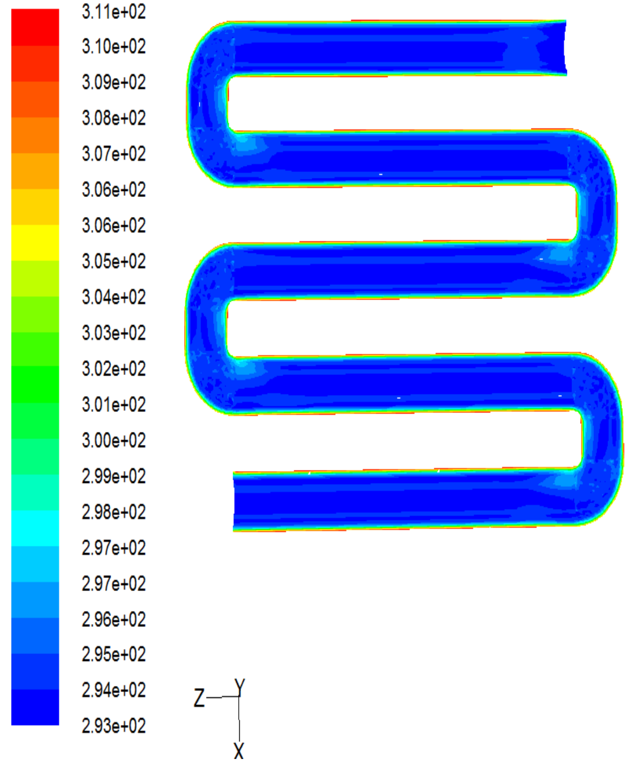

Inclined photo-reactor (α=45°)		Irradiation 780 W/m²
80 s	120 s	180 s

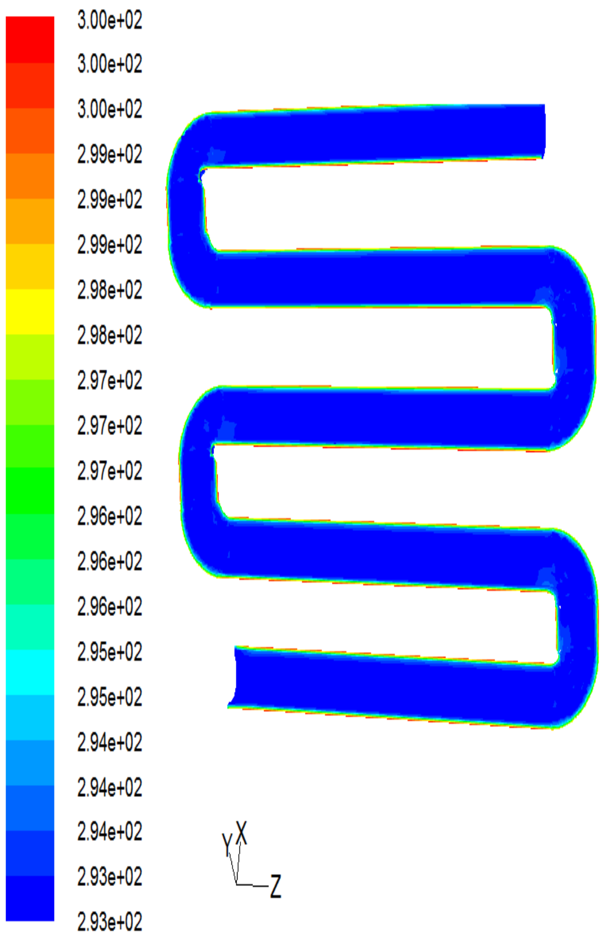

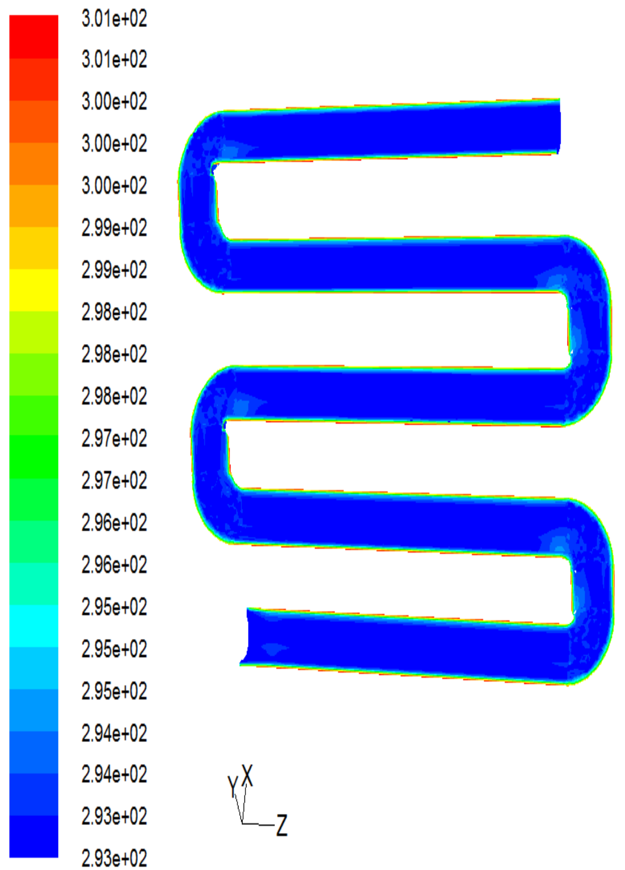

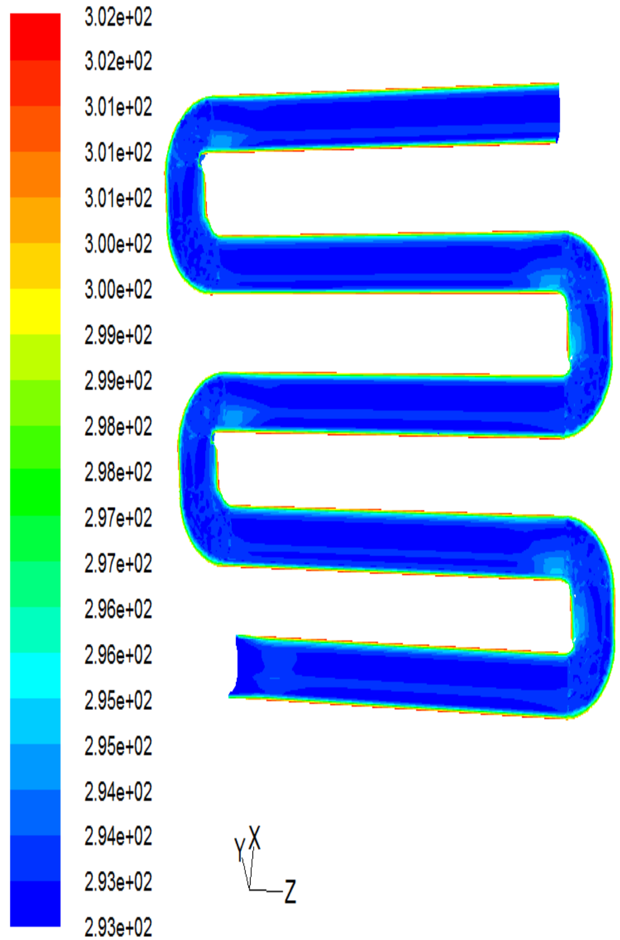

Inclined photo-reactor (α=45°)		Irradiation 1480 W/m²
80 s	120 s	180 s

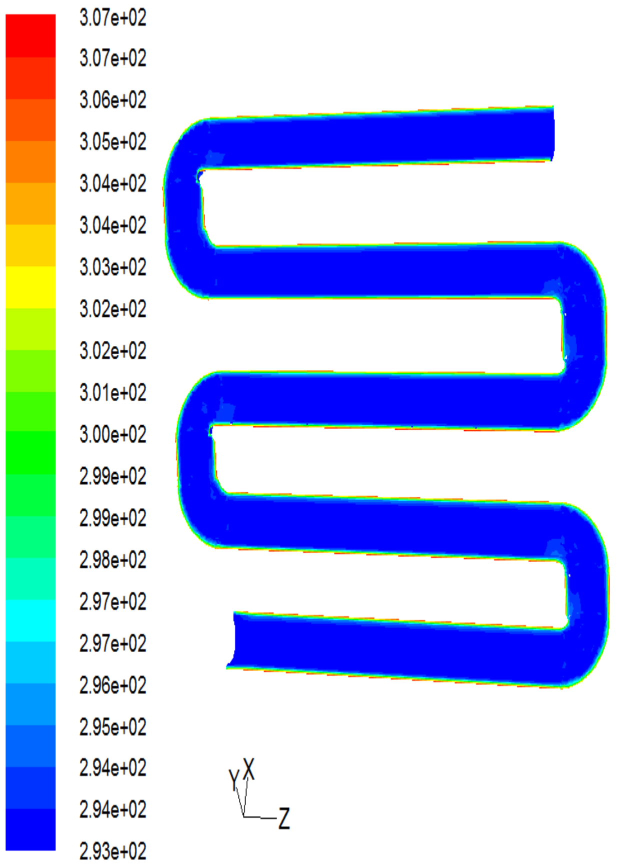

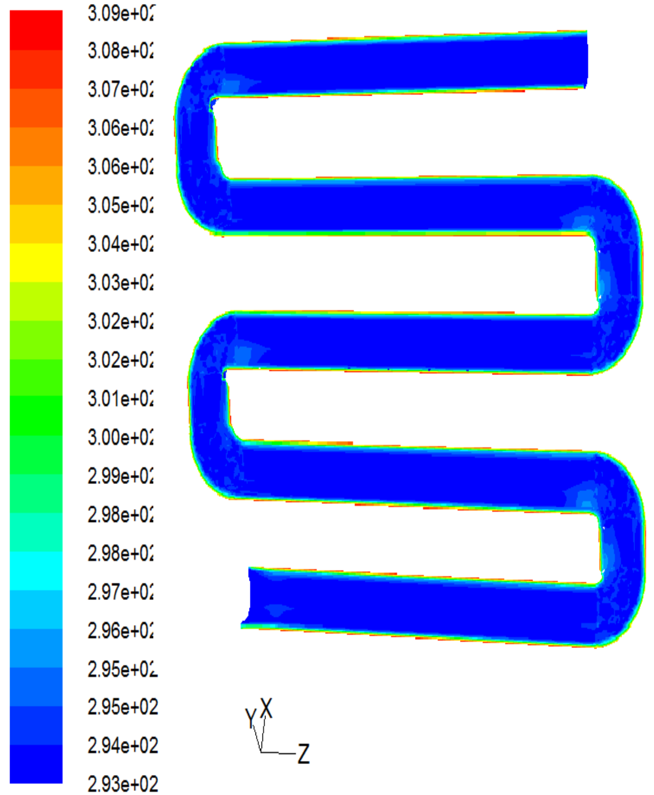

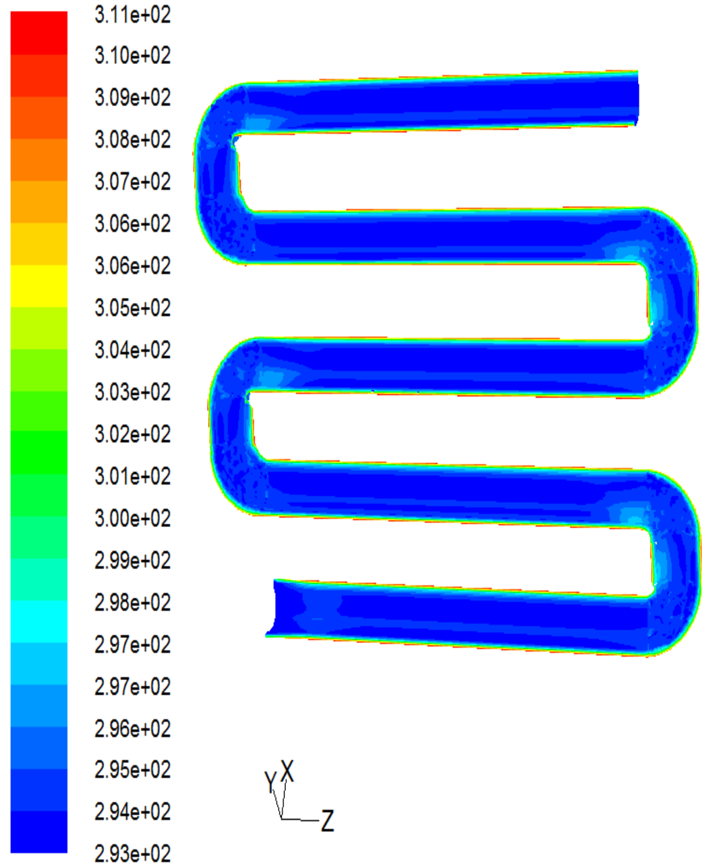

International Journal of Scientific Research and Management Studies (IJSRMS)
ISSN: 23493771 Volume 1 Issue 12, pg: 422-443

Inclined photo-reactor (α=36°)		Irradiation 780 W/m²
80 s	120 s	180 s
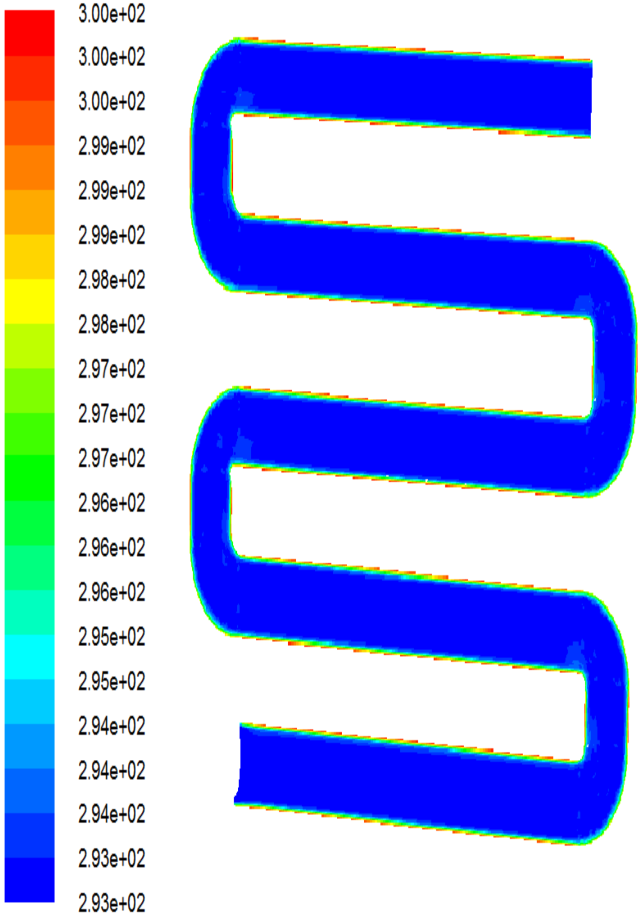	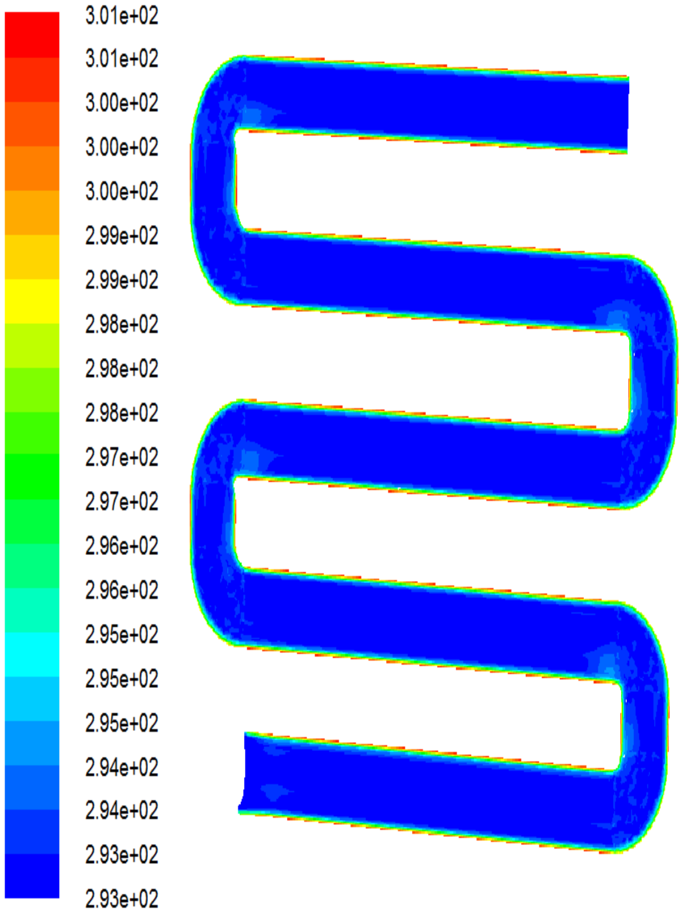	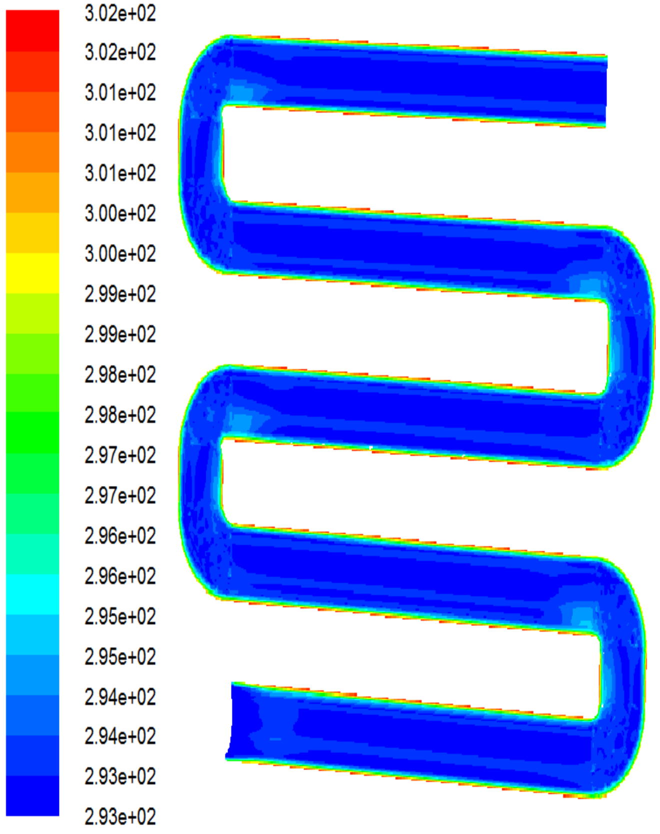

Inclined photo-reactor (α=36°)		Irradiation 1480 W/m²
80 s	120 s	180 s

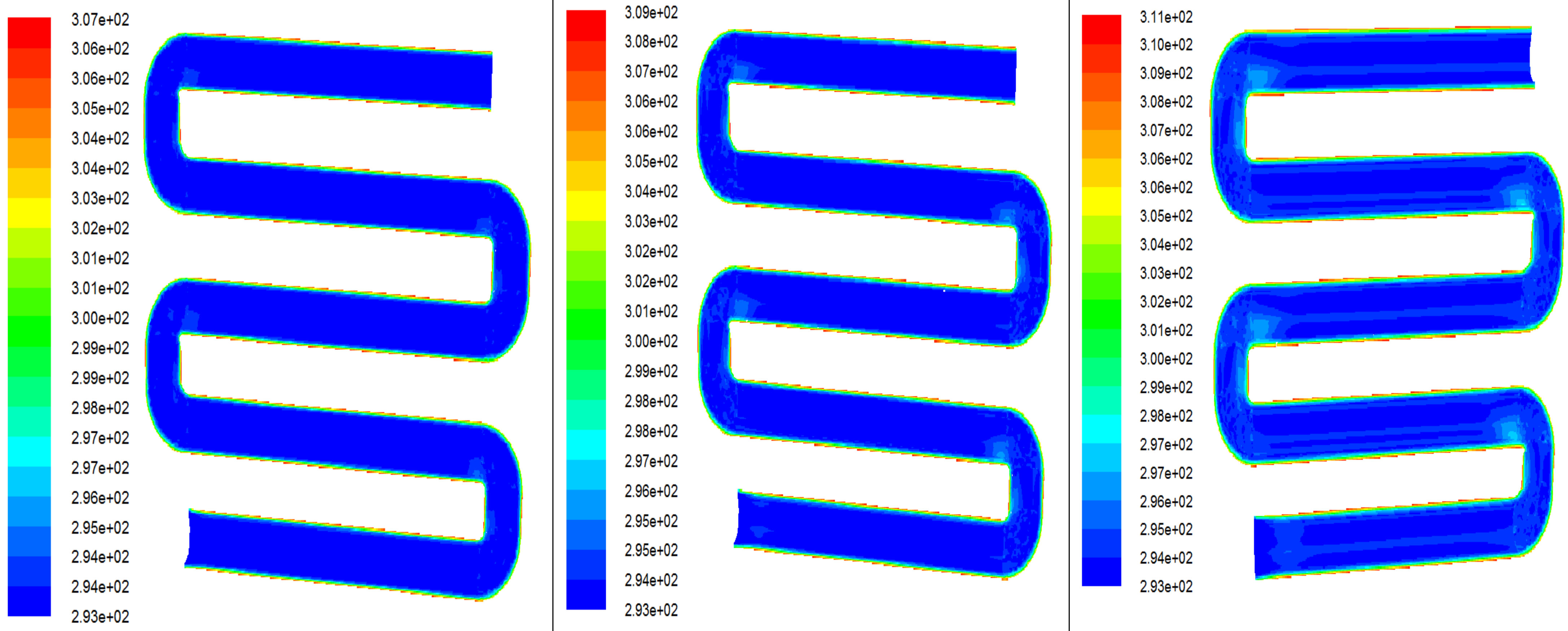

Figure4. Temperature fields

Curves of wastewater temperature as a function of solar irradiation intensity for horizontal and inclined photo-reactor are plotted on the figure below.

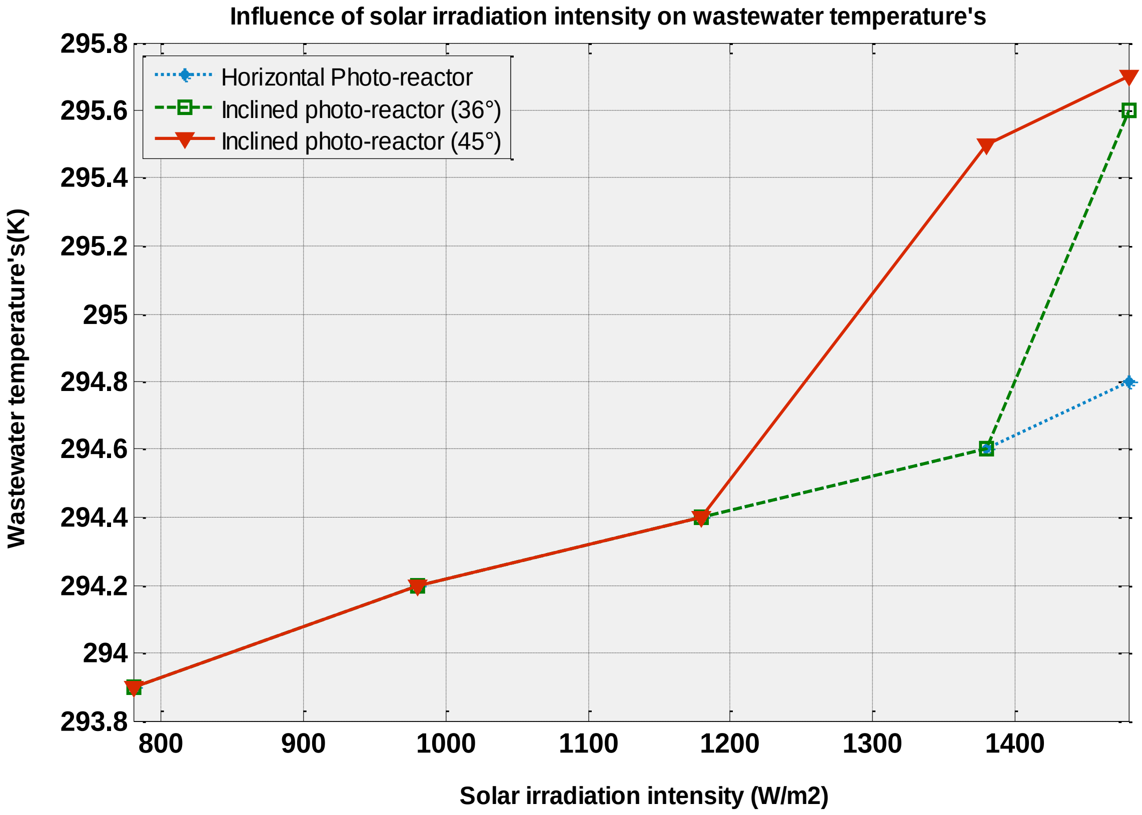

Figure 5. Wastewater temperature as function of incident radiation

For low values of solar irradiation intensity, inclination of photo-reactor has no effect on wastewater temperature until the three curves were superposed. But for high values, inclined photo-reactors show more sensitivity than horizontal photo-reactor.

4.3.4. Solar irradiation intensity distribution inside the tubular photo-reactor

The radiation model was activated in Fluent and the discrete ordinate method was selected. Intensity of irradiation ranges from: 780 to 1480 W/m^2**,** 1480 W/m^2 represents the maximal value of solar irradiation intensity measured the day of experimentation. Contours of incident radiation plotted below illustrate the presence of shadowed area both at horizontal and inclined reactors. This is due to the lack of radiation contribution from the dark sides which are elbows. It's clearly noted that distribution of solar irradiation is influenced by the inclination of reactor. In fact, for horizontal reactor, incident radiation is symmetric and high values focus at the middle of tubes. While for inclined photo-reactors, the lower parts of the tubes receive radiation dose much greater than other parts.

International Journal of Scientific Research and Management Studies (IJSRMS)
ISSN: 23493771 Volume 1 Issue 12, pg: 422-443

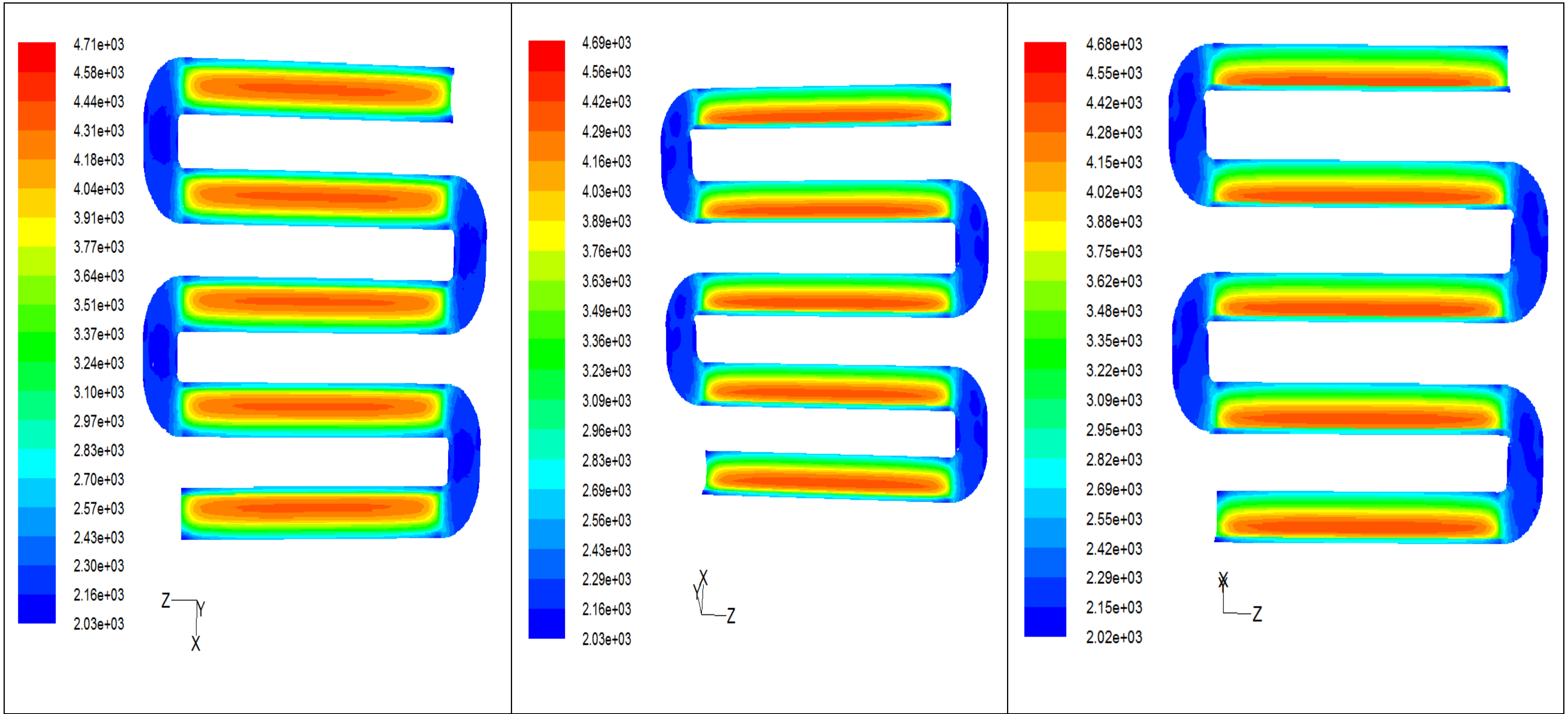

Horizontal Photo-reactor(α=0°)	Inclined Photo-reactor (α=36°)	Inclined Photo-reactor (α=45°)

Figure 6. Incident radiation

4.3.5. Velocity profile

Wastewater flow in the tubular photo-reactor was simulated with the Large Eddy Simulation. Figure below shows example of velocity magnitude profile for inclined reactor.

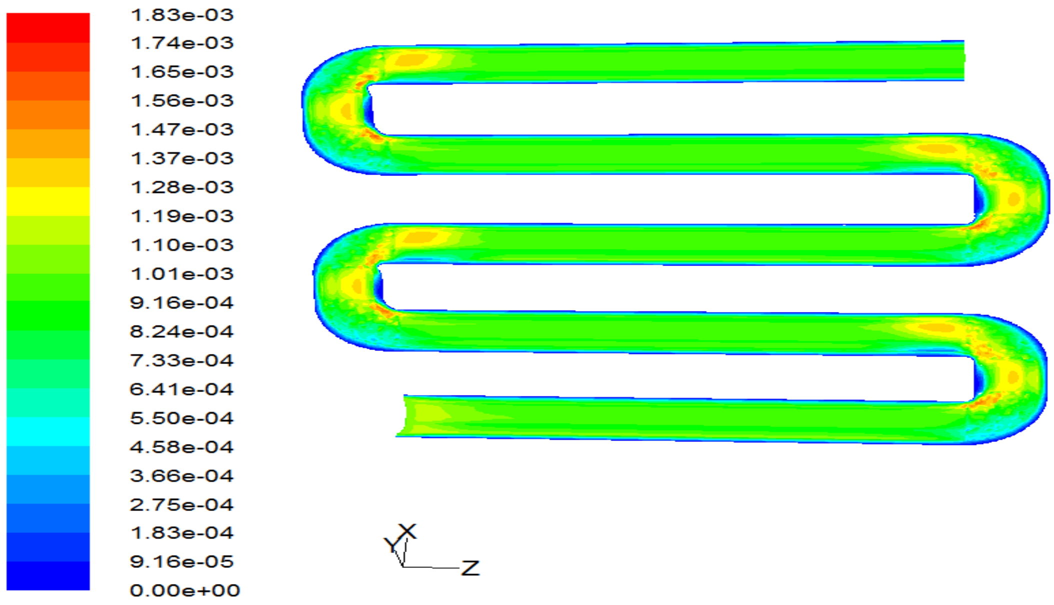

Figure 7. Velocity profile

According to these results, we note that water velocity field is homogeneous but a progressive increase of flow rate is observed at the elbow geometry. This is due to the effect of gravity and inclination position of reactor.

4.3.5. Turbulent viscosity

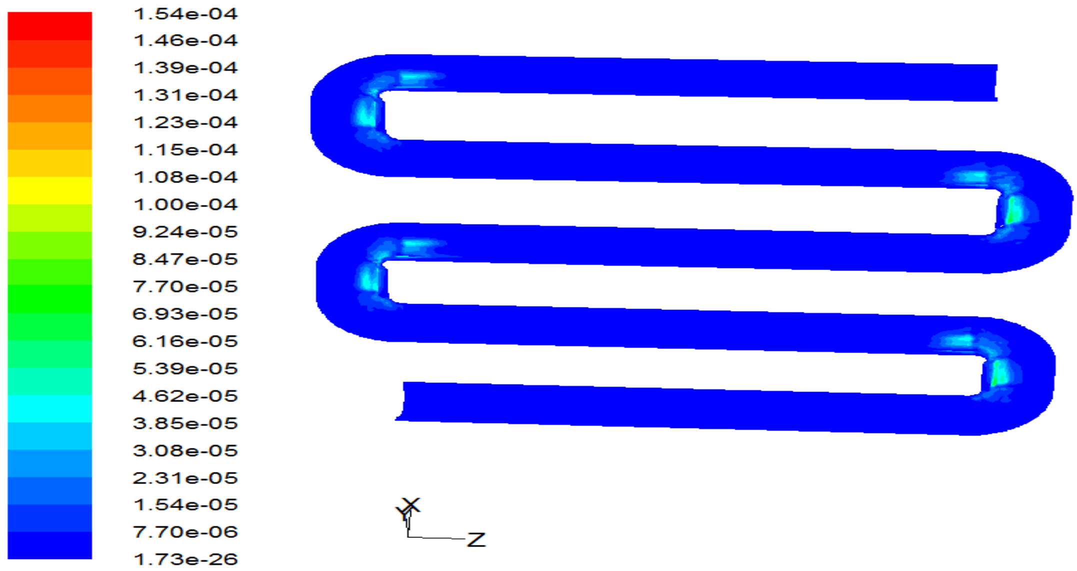

Figure 8. *Turbulent viscosity*

Figure above presents the distribution of the turbulent viscosity of the water flow. We note that there is a turbulence zones in elbow parts. We can explain that by the increasing in incident radiation which raise the fluid temperature and enhance the thermal viscosity, due to the presence of elbows in the photo-reactor geometry.

V. CONCLUSION AND FUTURE WORK

In this study we have interested to the simulation of hydrodynamic and incident radiation of tubular photo-reactor intended to waste water treatment by numerical software which is Fluent. The radiation model selected is the discrete ordinate method and hydrodynamic model is the Large Eddy Simulation. Simulation results obtained show that wastewater temperature depends on the intensity of solar irradiation and increases over exposure time for both horizontal and inclined photo-reactors. Distribution of solar irradiation is highly influenced by the inclination of reactor. In fact, for horizontal reactor, incident radiation is symmetric and high values focus at the middle of tubes . While for inclined photo-reactors, the lower parts of the tubes receive radiation dose much greater than other parts. Water velocity field is homogeneous but a progressive increase of flow rate is observed at the elbow geometry due to the effect of gravity and inclination position of reactor. Turbulence zones are presence in elbow parts of photo-reactor due to the increasing in incident radiation which raise the fluid temperature and enhance the thermal viscosity. This study should be accomplished by simulating the kinetic photo-chemical reaction and testing other inclination angle to optimize the incident radiation upon the reactor.

There are some limitations that should be noted and taken in to account when developing future related work.

First, insufficient data regarding the impact of radation on the global kinetic constant forced an internative process to adjust.to the selected power law model.

Second, strategies for accounting the turbulent mixture/ reaction in the chemical reaction step should be researched and implemented.

Finally, as regards to the model used, a 3D model would enable to the usage of fluent solar load as radiation source.

REFERENCES

[1]. Wastewater disinfection using UVA, UVC and solar radiations,Sadek Igoud, Fatiha Souahi, Chems Eddine Chitour, Lynda Amrouche, Chahinez Lamaa, Nadia Chekir, Amar Chouikh, 4ème Conference on Desalination and Water Treatment, Tunisia, 2013.

[2]. Some aspects of photocatalytic reactor modeling using computational fluid dynamics,Yash Boyjoo, Ming Ang, Vishnu Pareek, Chemical Engineering Science, 2012.

[3]. A numerical prediction on the reduction of microorganisms with UV disinfection, Chan Li, Baoqing Deng and Chang Nyung Kim, Journal of Mechanical Science and Technology, 2010.

[4]. Numerical simulation of an open channel ultraviolet wastewater disinfection reactor,Rajib Kumar Saha, thesis, 2013.

[5]. Modelling of UV disinfection reactors by means of Computational Fluid Dynamics, TU Wien, 2006.

[6]. Ultraviolet radiation and its germicidal effect in drinking water purification, K.M. Johnson, M.R. Anil Kumar, P. Ponmurugan and B. Mythili Gananamangai, Journal of Phytology, 2010.

[7]. Evaluation of Computational Fluid Dynamics (CFD) for Modeling UV-Initiated Advanced Oxidation Processes, Scott Michael Alpert, 2008.

[8]. Modeling virus transport and inactivation in a fluoropolymer tube UV photoreactor using Computational Fluid DynamicsFerdinando Crapulli, Domenico Santoro, Charles N. Haas, Michele Notarnicola, Lorenzo Liberti Chemical Engineering Journal 161 (2010) 9–18.

[9]. Thermal Modelling of Green Roofed Urban Buildings, Sadiq Abubakar Gulma, Patrick Ajwang and Stephen N. Ondimu, International Journal of Advances in Engineering & Technology, Vol. 7, Issue 4, pp. 1179-1190, Sept., 2014.

[10]. CFD modeling of a UV-LED photocatalytic odor abatement process in a continuous reactorZimeng Wang, Jing Liu, Yuancan Dai, Weiyang Dong, Shicheng Zhang, Jianmin ChenJournal of Hazardous Materials 215– 216 (2012) 25– 31.

[11]. Computational Fluid Dynamics (CFD) Modeling.Christopher RiffLPPD-Project 12/31/04.
[12]. APPLICATION of COMPUTATIONAL FLUID DYNAMICS to the DESIGN of PHOTOCATALYTIC REACTORS. Workshop on Nanomaterials for Photocatalytic Depollution. Javier Marugán. Workshop on Nanomaterials for Photocatalytic Depollution. 22January, 2014
[13]. Computational Fluid Dynamics Based Models for Assessing UV Reactor Design and Installation. Water Research Foundation. ALL RIGHTS RESERVED.2012
[14]. Mills, A.; R. H. Davies and D. Worsley. Water purification by semiconductor photocatalysis. Chem. Soc. Rev., *22*, pp.417-426. 1993.
[15]. M.L. Thompson, H.T. Bi, and J.R. Grace, A generalized bubbling/turbulent fluidized bed reactor model, Chemical Engineering Science, 54, 5175 –5185, 1999.
[16]. B.N. Murthy, R.S. Ghadge, and J.B. Joshi, CFD simulations of gas–liquid–solid stirred reactor: Prediction of critical impeller speed for solid suspension, Chem Eng Science., 62, 7184-7915, 2007.

Authors Biography

AOUDJIT Lamine, received the master degree in organic chemical from University USTHB, Algeria. He is presently doing his research work at Unit Development of Solar Equipment (UDES), His research interests is in renewable energies and wastewater treatment using photocatalysis process.

SEBTI Aicha is PhD student in Chemical Engineering in the Polytechnic School of Algeria, working under the supervision of Professor SOUAHI Fatiha. Her main research interests are water treatment technology with renewable energy as well as the assessment of water quality.

Farid Madjene received the master degree in Environmental Engineering from University USTHB, Algeria His research interests' water treatment technology with renewable energy.

Hafida Lebik is PhD student in Environmental Engineering in the University of Science and Technology Houari Boumediene, working under the supervision of Professor Aït-Amar Hamid. Her main research interests are water treatment technology with renewable energy as well as the assessment of water quality. Additionally, she studies the impact of pesticides use on groundwater.

Belgassim Boutra is PhD student in Environmental Engineering in the University of Science and Technology Houari Boumediene, Her main research interests are water treatment.

IGOUD Sadek is PhD student in Chemical Engineering in the Polytechnic School of Algeria, working under the supervision of Professor SOUAHI Fatiha. His main research interests are water treatment technology with renewable energy as well as the assessment of water quality.